

# The Postcollapse Equilibrium Structure of Cosmological Haloes in a Low-Density Universe

Ilian T. Iliev<sup>1,2</sup> and Paul R. Shapiro<sup>3</sup>

<sup>1</sup>*Dept. of Physics, The University of Texas at Austin, Austin, TX 78712, USA*

<sup>2</sup>*Instituto de Astronomía-Universidad Nacional Autónoma de México, Apdo Postal 70-264, 04510 México D.F., México,*

*E-mail: iliev@astrocu.unam.mx*

<sup>3</sup>*Dept. of Astronomy, The University of Texas at Austin, Austin, TX 78712, USA, E-mail: shapiro@astro.as.utexas.edu*

1 December 2018

## ABSTRACT

An analytical model is presented for the postcollapse equilibrium structure of virialized objects which condense out of a low-density cosmological background universe, either matter-dominated or flat with a cosmological constant. This generalizes the model we derived previously for an Einstein-de Sitter (EdS) universe. The model is based upon the assumption that cosmological haloes form from the collapse and virialization of “top-hat” density perturbations and are spherical, isotropic, and isothermal. This leads to the prediction of a unique, nonsingular, truncated isothermal sphere (TIS), a particular solution of the Lane-Emden equation (suitably modified when  $\Lambda \neq 0$ ). The size and virial temperature are unique functions of the mass and redshift of formation of the object for a given background universe. The central density is roughly proportional to the critical density of the universe at the epoch of collapse. This TIS model is in good agreement with observations of the internal structure of dark matter-dominated haloes on scales ranging from dwarf galaxies to X-ray clusters. It also reproduces many of the average properties of haloes in simulations of the Cold Dark Matter (CDM) model to good accuracy, suggesting that it is a useful analytical approximation for haloes which form from realistic initial conditions. Our TIS model matches the density profiles of haloes in CDM N-body simulations outside the innermost region, while avoiding the steep central cusp of the latter which is in apparent con-

flict with observations. The TIS model may also be relevant to nonstandard CDM models, like self-interacting dark matter, recently proposed to resolve this conflict.

**Key words:** cosmology: theory – dark matter – galaxies: clusters: general – galaxies: formation – galaxies: haloes – galaxies: kinematics and dynamics

## 1 INTRODUCTION

Galaxies and clusters of galaxies formed when gravitational instability amplified density fluctuations in the expanding cosmological background universe. Regions denser than average eventually stopped expanding and recollapsed to form virialized objects. The question of what equilibrium structure results when a density perturbation collapses out of the expanding background universe and virializes is central to the theory of galaxy formation. The nonlinear outcome of the growth of Gaussian-random-noise cosmological density fluctuations due to gravitational instability in a hierarchical clustering model like CDM is not amenable to direct analytical solution, however. Instead, numerical simulations are required. As a guide to understanding these simulations, as a check on their accuracy, and as a means of extrapolating from simulation results of limited dynamic range, analytical approximations are nevertheless an essential tool. One such tool of great utility has been the solution of the spherical top-hat perturbation problem (e.g. Peebles 1980, Padmanabhan 1993). As used in the Press-Schechter (“PS”) approximation (Press & Schechter 1974) and its various refinements, the top-hat model serves to predict well the number density of virialized haloes of different mass which form at different epochs in N-body simulations. An analytical model for the internal structure (e.g. mass profile, temperature, velocity dispersion, radius) of these virialized haloes would be a further tool of great value for the semi-analytical modelling of galaxy and cluster formation, therefore. Shapiro, Iliev & Raga (1998; Paper I) derived such a model for an EdS universe. Here we shall generalize the analysis of Paper I to the case of a low-density universe ( $\Omega_0 < 1$ ) which is either matter-dominated or flat with a cosmological constant (i.e.  $\Omega_0 = 1 - \lambda_0$ ). We shall also describe how the TIS model can be generalized to other cosmologies with a nonclumping background component, such as quintessence.

It is generally assumed that the collapse to infinite density predicted by the exact, nonlinear solution of the spherical top-hat perturbation problem is interrupted by a violent

relaxation to virial equilibrium at a finite density, as a result of the growth of initially small-amplitude inhomogeneities in the density distribution. Earlier work adopted the crude approximation that the postcollapse object which emerges from this violent relaxation is either a uniform sphere or a singular isothermal sphere, with the same total mass and energy as the collapsing top-hat and with a radius and velocity dispersion (or, equivalently, gas temperature) fixed in accordance with the virial theorem. Our first motivation, therefore, was simply to improve upon this earlier treatment by finding a more realistic outcome for the top-hat problem. As a starting point, we adopted the assumption that the final equilibrium is spherical, isotropic, and isothermal, a reasonable first approximation to the N-body and gasdynamic simulation results of the CDM model. The postcollapse analytical solution we derived in Paper I from this assumption quantitatively reproduces many of the average properties of the haloes found in those simulations to good accuracy, so we are encouraged to believe that our approximation is well justified for haloes which form from realistic initial conditions. Our model is in disagreement, however, with one detail of the N-body simulation results that, in their very centers, simulated haloes have cuspy profiles (e.g. Navarro, Frenk & White 1997; “NFW”). By contrast, our model predicts a density profile with a small, uniform-density core, in good agreement with the observed rotation curves of dark matter-dominated galaxies (Iliev and Shapiro 2001) and with cluster mass profiles inferred from gravitational lensing (Iliev and Shapiro 2000, Shapiro and Iliev 2000). This apparent discrepancy between the cuspy profiles of the N-body results and the observed dark matter-dominated haloes (e.g. Moore et al. 1999) has led recently to a vigorous reexamination of the cold, collisionless nature of CDM, itself, and the suggestion that a variation of the microphysical properties of the dark matter might make it more “collisional”, enabling it to relax dynamically inside these haloes so as to eliminate the central cusp (e.g. Spergel & Steinhardt 2000; Burkert 2000; Davè et al. 2000, Firmani et al. 2000 and references therein). While the details of this suggestion are still uncertain, our model can also be applied in that case, to the extent that we are able to ignore the details of the relaxation process inside the halo and approximate the final equilibrium as isothermal.

As described in Paper I, our model is as follows: An initial top-hat density perturbation collapses and virializes, which leads to a truncated nonsingular isothermal sphere in hydrostatic equilibrium (TIS), a solution of the isothermal Lane-Emden equation. Although

the mass and total energy of the top-hat are conserved thru collapse and virialization, and the postcollapse temperature is set by the virial theorem (including the effect of a finite boundary pressure), the solution is not uniquely determined by these requirements alone. In order to find a unique solution, some additional information is required. We adopted the ansatz that the solution selected by nature is the “minimum-energy solution” such that the boundary pressure is that for which the conserved top-hat energy is the minimum possible for an isothermal sphere of fixed mass within a finite truncation radius. This assumption fixes the ratio of the radius of the postcollapse sphere to the radius of the top-hat perturbation which created it, as measured at the latter’s epoch of maximum expansion, uniquely. For comparison, we appealed to the details of the exact, self-similar, spherical, cosmological infall solution of Bertschinger (1985). In this solution, an initial overdensity causes a continuous sequence of spherical shells of cold matter, both pressure-free dark matter and baryonic fluid, centered on the overdensity, to slow their expansion, turn around and recollapse. The baryonic infall is halted by a strong accretion shock, while density caustics form in the collisionless dark matter, instead, due to shell-crossing. The postcollapse, virialized object we wish to model is then identified with the spherical region of shell-crossing dark matter and shock-bounded baryonic fluid in this infall solution (for ratio of specific heats  $\gamma = 5/3$ ) for which the mass is the same as that of our top-hat and the trajectory of its outermost spherical mass shell was identical to that of the outer boundary of our collapsing top-hat at all times until it encountered the shock. According to the detailed similarity solution for this infall problem, this spherical region of post-shock gas and shell-crossing dark matter, it turns out, is very close to hydrostatic and isothermal and has virtually the same radius as that of the minimum-energy solution for the matching TIS. This offers some support for our “minimum-energy” ansatz and explains the dynamical origin of the boundary pressure as that which results from thermalizing the kinetic energy of infall.

With this “minimum-energy” ansatz, we found that top-hat perturbation collapse leads to a unique, nonsingular TIS, which yields a universal, self-similar density profile for the postcollapse equilibrium of virialized cosmological haloes. Our solution has a unique length scale and amplitude set by the top-hat mass and collapse epoch, with a density at every point which is proportional to the background density at that epoch. The density profiles for gas and dark matter are assumed to be the same (no bias). The final virialized halo has

a small but flat-density core. For the EdS case, this core radius  $r_0$  is about 1/30 of the total size  $r_t$  of the halo (i.e. the truncation radius). [We note that this core radius  $r_0 \equiv r_{0,\text{King}}/3$ , where  $r_{0,\text{King}}$  is the “King radius” defined by Binney & Tremaine (1987, equ. [4-124b])]. The central density  $\rho_0$  is about 500 times the density  $\rho_t$  at the surface and 18,000 times the background density at the collapse epoch. At intermediate radii,  $\rho$  drops faster than  $r^{-2}$ , as fast as  $r^{-2.5}$ . The one-dimensional velocity dispersion  $\sigma_V$  of the dark matter and the gas temperature  $T$  are given simply by  $\sigma_V^2 = k_B T / m = 4\pi G \rho_0 r_0^2$ , where  $m$  is the mean gas mass per gas particle. This temperature is significantly different from that predicted by the standard uniform sphere (SUS) and singular isothermal sphere (SIS) approximations adopted previously in the literature, with  $T = 2.16 T_{\text{SUS}} = 0.72 T_{\text{SIS}}$ .

The derived mass profile of our TIS solution as a function of its virial temperature (or velocity dispersion) and its formation epoch reproduces to remarkably high accuracy (i.e. of order 1%) the cluster mass-radius-temperature relationships and average mass profile for CDM haloes which Evrard, Metzler, and Navarro (1996) derived empirically by fitting a large set of detailed numerical gas dynamical and N-body simulation results of cluster formation in the CDM model. The TIS and NFW halo mass profiles are also in very close agreement (fractional deviation of less than  $\sim 10\%$ ) at all radii outside of a few TIS core radii (i.e. about one King radius) for NFW concentration parameters  $4 \leq c_{\text{NFW}} \leq 7$ . In short, our TIS model is in good agreement with the average properties of simulated CDM haloes although it differs from these numerical results at very small radii.

The purpose of this paper is to generalize the results of Paper I to the case of a low-density universe, either open and matter-dominated ( $\Omega_0 < 1$ ,  $\lambda_0 = 0$ ), or flat with cosmological constant ( $\Omega_0 = 1 - \lambda_0$ ). In the former case, the internal structure of the TIS haloes will be the same as for the EdS results of Paper I, when radius and density are expressed in dimensionless terms in units of the core radius and central density. However, these latter dimensional quantities will be functions of the total mass and the formation epoch of the halo, functions which differ from the EdS results and depend upon the value of  $\Omega_0$ . These differences between the EdS solution for the TIS model in Paper I and that presented here for the open, matter-dominated universe ( $\Omega_0 < 1$ ) can be understood as a reflection of the different solutions for the spherical top-hat problem in the two cases. For the case with a cosmological constant, however, the differences with respect to the EdS solution are much

more extensive. In this case, not only is it necessary to consider the differences which result from the different solution for the spherical top-hat problem, but it is also necessary to take proper account of nonzero  $\Lambda$  in the virial theorem, the conservation of energy, and the isothermal Lane-Emden equation, as well. In § 2, we shall summarize the spherical top-hat perturbation problem generalized to these low-density Friedmann universe cases. We will also briefly describe how the conservation of energy and the virial theorem are generalized in the presence of some uniform background component  $X$  of energy density, such as the cosmological constant or quintessence, and how these are combined with the top-hat solution to derive the properties of the postcollapse virialized object when the latter is assumed to be a uniform sphere [i.e. the “standard uniform sphere approximation” in the presence of the  $X$ -component]. We will then specialize these general results to the case in which the uniform component  $X$  is the cosmological constant. In § 3, we will generalize the Lane-Emden equation for an isothermal sphere in hydrostatic equilibrium to take account of the presence of the  $X$ -component and specialize our discussion of its solutions to the cosmological constant case. In § 4, we shall apply the virial theorem to these generalized isothermal Lane-Emden spheres, taking care to account properly for the important effect of finite boundary pressure. In § 5, we will derive the minimum-energy TIS solutions for these low-density universe cases, including convenient analytical fitting formulae for practical application, in which all properties of the virialized post-collapse object are given as explicit functions of the mass and collapse redshift of the object for a given background cosmology. Our results and conclusions are summarized in § 6, where we compare the TIS solutions for low-density universes derived here with the SUS and SIS approximations for those cases, as well as with the TIS solution of Paper I for the EdS case. Finally, in view of the suggestive physical correspondence between our TIS solution in the EdS case and the shock- and caustic-bounded sphere in the self-similar, spherical infall solution of Bertschinger (1985), we have added an Appendix A in which we show how the latter solution (for an EdS universe) can also be applied at early times in the generalized low-density universe cases described here, by a simple rescaling of parameters.

## 2 SPHERICAL TOP-HAT PERTURBATIONS IN A LOW-DENSITY FRIEDMANN UNIVERSE AND THE STANDARD UNIFORM SPHERE APPROXIMATION

### 2.1 Before Collapse: the Exact Nonlinear Solution

The spherical top-hat model, an uncompensated spherical perturbation of uniform overdensity within a finite radius (Gunn & Gott 1972), affords considerable insight into the dynamics of the gravitational growth of cosmic structure, while still having an exact, analytical or semi-analytical solution (e.g. Peebles 1980). In what follows, we shall consider top-hat perturbations in cosmological models with two components: (1) a nonrelativistic component, which comprises all forms of matter, luminous or dark, baryonic or non-baryonic, that can cluster under the action of gravity, and (2) a uniform component, which does not clump at any scale of interest. As a special case we shall consider low-density matter-dominated universes with no uniform component, as well.

The equation of state of the uniform component X relates its pressure  $p_X$  to its energy-density  $\rho_X$  according to

$$p_X = \left(\frac{n}{3} - 1\right) \rho_X c^2 \equiv w \rho_X c^2. \quad (1)$$

Let us also define the quantity

$$\rho_{X,\text{eff}} \equiv \rho_X + 3p_X/c^2 = (1 + 3w)\rho_X = (n - 2)\rho_X. \quad (2)$$

The mean rest mass energy density  $\rho_b$  of the nonrelativistic component and the energy density  $\rho_X$  then each vary with time according to

$$\rho_b(t) \propto a(t)^{-3}, \quad (3)$$

$$\rho_X(t) \propto a(t)^{-n}, \quad (4)$$

where  $a(t)$  is the Robertson-Walker scale factor, and  $n$  is a non-negative constant. [For details and references, see e.g. Martel & Shapiro (1998), and Wang & Steinhardt (1998)]. Particular values of  $n$  correspond to models with a nonzero cosmological constant ( $n = 0$ ,  $w = -1$ ), domain walls ( $n = 1$ ,  $w = -2/3$ ), string networks ( $n = 2$ ,  $w = -1/3$ ), vacuum stress or massive neutrinos ( $n = 3$ ,  $w = 0$ ), radiation background ( $n = 4$ ,  $w = 4/3$ ), and quintessence ( $0 \leq n < 3$ ,  $-1 \leq w < 0$ ).

The time-evolution of the scale factor  $a(t)$  is described by the Friedmann equation. For the two-component models considered here, this equation takes the form

$$\left(\frac{\dot{a}}{a}\right)^2 \equiv H(t)^2 = H_0^2 \left[ (1 - \Omega_0 - \Omega_{X,0}) \left(\frac{a}{a_0}\right)^{-2} + \Omega_0 \left(\frac{a}{a_0}\right)^{-3} + \Omega_{X,0} \left(\frac{a}{a_0}\right)^{-n} \right], \quad (5)$$

where  $H(t)$  is the Hubble parameter, the density parameters of the nonrelativistic matter and X components are  $\Omega = \rho_b/\rho_{\text{crit}}$  and  $\Omega_X = \rho_X/\rho_{\text{crit}}$ , respectively, where  $\rho_{\text{crit}} = 3H^2(t)/8\pi G$ , and all subscripts “0” refer to present values. The redshift  $z$  that corresponds to a scale factor  $a(t)$  is given by the usual relation

$$1 + z = \frac{a_0}{a(t)}. \quad (6)$$

In what follows, it will be convenient to define the scale factor at present by

$$a_0 \equiv \begin{cases} \left(\frac{\Omega_{X,0}}{\Omega_0}\right)^{1/(3-n)}, & \rho_X \neq 0; \\ 1, & \text{matter-dominated, } \Omega_0 = 1; \\ \frac{1 - \Omega_0}{\Omega_0}, & \text{matter-dominated, } \Omega_0 < 1. \end{cases} \quad (7)$$

While the X-component does not clump under the force of gravity, its presence not only affects the the rate of expansion of the universe as indicated by equation (5); it also modifies the gravitational forces on the matter component, as follows. The Poisson equation in the presence of this non-clumping component is

$$\nabla^2 \Phi_{\text{tot}} = 4\pi G(\rho + \rho_{X,\text{eff}}), \quad (8)$$

and the corresponding gravitational potential is

$$\Phi_{\text{tot}} = \Phi + \frac{2\pi G \rho_{X,\text{eff}} r^2}{3} \equiv \Phi + \Phi_X, \quad (9)$$

where  $\Phi$  is the gravitational potential due to the nonrelativistic matter component as it would be in the absence of the X-component, and  $\Phi_X$  is the correction due to the X-component. From Birkhoff’s theorem, the collapse of a spherical top-hat density perturbation can be described by the Friedmann equation for a universe with a higher average density than that of the background universe outside the top-hat. Special cases of the top-hat model in universes with a nonclumping component were discussed in Lahav et al. (1991) (for the cosmological constant), and Wang & Steinhardt (1998) (for quintessence). Here we shall only give the basic equations and refer the reader to these papers for further details and references.

The density inside the top-hat stays uniform during collapse. We can, therefore, describe



its evolution solely in terms of its overdensity  $\delta$  with respect to the background. The equation for the evolution of the top-hat overdensity in the presence of a nonclumping component with  $n < 3$  is (Shapiro, Martel, and Iliev 2001)

$$\frac{d^2 \ln(\delta + 1)}{d \ln a^2} - \frac{1}{3} \left( \frac{d \ln(\delta + 1)}{d \ln a} \right)^2 + \frac{g_1}{g_2} \frac{d \ln(\delta + 1)}{d \ln a} - \frac{3(\delta + 1)}{g_2} = 0, \quad (10)$$

where

$$g_1 \equiv 2\kappa a + 1 + (4 - n)a^{3-n}, \quad g_2 \equiv 2(\kappa a + 1 + a^{3-n}), \quad \kappa \equiv \frac{(1 - \Omega_0 - \Omega_{X,0})\Omega_0^{(n-2)/(3-n)}}{\Omega_{X,0}^{1/(3-n)}}. \quad (11)$$

The boundary conditions are given by

$$\delta(0) = 0, \quad \frac{d\delta}{da}(0) = A, \quad (12)$$

where  $A$  indicates the initial amplitude of the top-hat fluctuation. For  $\kappa=0$ , the solution  $\delta(a)$  of equation (10) is independent of  $\Omega_0$  and  $\Omega_{X,0}$ . In that case, we need solve equation (10) only once to obtain the family of solutions for different  $\Omega_0$ . For open, matter-dominated models, equation (10) is replaced by

$$\frac{d^2 \ln(\delta + 1)}{d \ln a^2} - \frac{1}{3} \left( \frac{d \ln(\delta + 1)}{d \ln a} \right)^2 + \frac{2a + 1}{2(a + 1)} \frac{d \ln(\delta + 1)}{d \ln a} - \frac{3\delta}{2(a + 1)} = 0 \quad (13)$$

(Shapiro et al. 2001).

Let us define the critical density contrast  $\delta_{\text{crit}}$  as the solution  $\delta_L$  of the linearized version of equation (10) or equation (13), extrapolated to the epoch at which the nonlinear solution  $\delta$  predicts an infinite overdensity. This quantity  $\delta_{\text{crit}}$  labels the time of collapse in scale-free units. The values obtained at turnaround will be denoted by subscript “ $m$ ” for “maximum expansion,” while the values at collapse time will be denoted by subscripts “coll”. Henceforth, we shall refer to  $z_{\text{coll}}$  as the redshift which corresponds to the epoch of infinite collapse, at which  $\delta = \infty$ , at time  $t_{\text{coll}}$ .

## 2.2 After Collapse: The Standard Uniform Sphere Approximation

The properties of the final, virialized object which is postulated to result from top-hat collapse were derived in the “standard uniform sphere approximation” for the case with a cosmological constant by Lahav et al. (1991) and for the case of quintessence by Wang & Steinhardt (1998). The postcollapse state is fully described in this approximation by the radius and internal velocity dispersion of the final equilibrium sphere.

The SUS approximation assumes that the collapse of the top-hat to infinite density is interrupted by a rapid equilibration when  $\delta_L = \delta_{\text{crit}}$ , which results in another uniform sphere in virial equilibrium. The final radius  $r_{\text{vir}}$  of the virialized sphere is obtained by assuming that the energy of the top-hat is conserved during collapse and virialization and applying the virial theorem to the final state, assuming that the boundary pressure term in the virial theorem can be neglected. The conserved total energy of the sphere is  $E = K + W_{\text{tot}}$ , where  $K = U_{\text{th}} + T_{\text{kin}}$ ,  $U_{\text{th}}$  and  $T_{\text{kin}}$  are the thermal and kinetic energy, respectively,

$$W_{\text{tot}} = \frac{1}{2} \int_V \rho \nabla \Phi_{\text{tot}} \cdot \mathbf{r} dV \equiv W + W_X \quad (14)$$

is the total potential energy in the presence of the X-component, the terms  $W$  and  $W_X$  are defined by the integral expression in equation (14) with  $\Phi$  and  $\Phi_X$ , respectively, and  $\Phi_{\text{tot}}$ ,  $\Phi$  and  $\Phi_X$  are defined by equation (9).

Let us define the collapse factor which relates the size of the sphere at maximum expansion  $r_m$  to its postcollapse equilibrium size  $r_{\text{vir}}$  as  $\eta \equiv r_{\text{vir}}/r_m$ . The relative gravitational importance of the X-component and the matter component at maximum expansion are indicated by the dimensionless ratio  $\theta \equiv -(\rho_{\text{X,eff}}/2\rho)_m$ , where  $\rho$  is the matter density inside the top-hat. At the point of maximum expansion [which, unlike the EdS case, exists only for top-hat perturbations of amplitude high enough to enable collapse (see, for example, Martel 1994)], the sphere is cold and at rest, so  $K = 0$ , and its energy consists entirely of gravitational potential energy. For a uniform sphere of mass  $M_0$  and radius  $r_m$ , equations (9) and (14) yield

$$E = (W + W_X)_m = -\frac{3}{5} \frac{GM_0^2}{r_m} \left(1 - \frac{\rho_{\text{X,eff}}}{2\rho}\right)_m = -\frac{3}{5} \frac{GM_0^2}{r_m} (1 + \theta). \quad (15)$$

After collapse, when the system settles down to a virial equilibrium, the total potential energy is

$$(W + W_X)_{\text{vir}} = -\frac{3}{5} \frac{GM_0^2}{r_{\text{vir}}} \left(1 - \frac{\rho_{\text{X,eff}}}{2\rho}\right)_{\text{vir}} = -\frac{3}{5} \frac{GM_0^2}{r_{\text{vir}}} \left[1 + \theta \eta^3 \left(\frac{a_{\text{coll}}}{a_m}\right)^{-n}\right], \quad (16)$$

where  $a_m$  is the scale factor at turnaround and  $a_{\text{coll}}$  is the scale factor at collapse. According to the virial theorem, the kinetic and gravitational potential energies are related at this epoch by

$$3(\gamma - 1)K + W - 2W_X = 0, \quad (17)$$

where  $\gamma$  is the ratio of specific heats. We take  $\gamma = 5/3$ . Together with the conservation of

energy, this implies that  $E = W/2 + 2W_X$ , and, therefore, the total energy in equation (15) is related to the virial radius and densities after collapse according to

$$E = -\frac{3}{10} \frac{GM_0^2}{r_{\text{vir}}} \left( 1 - \frac{2\rho_{X,\text{eff}}}{\rho} \right)_{\text{vir}}. \quad (18)$$

Equating the total energy  $E$  in equations (15) and (18) and using equation (4) then yields an equation for the collapse factor  $\eta$ ,

$$4\theta\eta^3 \left( \frac{a_{\text{coll}}}{a_m} \right)^{-n} - 2(1 + \theta)\eta + 1 = 0. \quad (19)$$

Hereafter we shall limit our discussion to the case  $n = 0$  (cosmological constant), with open, matter-dominated models as a limiting case for which  $\rho_{X,\text{eff}} = 0$ . Equation (19) then becomes

$$4\theta\eta^3 - 2(1 + \theta)\eta + 1 = 0, \quad (20)$$

where  $\theta = \rho_\lambda/\rho_m$  and  $\rho_\lambda$  is the constant vacuum energy density associated with the cosmological constant [i.e.  $\rho_\lambda = \Lambda/(8\pi G)$ ]. For any matter-dominated universe,  $\theta = 0$  and equation (20) reduces to the well-known relation  $\eta = 1/2$ . In general, equation (20) has a closed form solution  $\eta(\theta)$ . However the expression is quite complicated and not very practical. Instead, simpler, approximate solutions have been proposed (Lahav et al. 1991, Kochanek 1995). We have derived our own, better approximation to the exact solution [with an error of order  $O(\theta^5)$ ]:

$$\eta = 0.5 - 0.25\theta - 0.125\theta^2 + 0.125\theta^3 + 0.21875\theta^4. \quad (21)$$

The upper limit for the  $\theta$  parameter is  $1/2$ . If  $\theta > 1/2$ , then the right hand side of equation (8) evaluated at the epoch of maximum expansion would be negative, and, therefore, the perturbation would not be bound. For  $\theta \rightarrow 1/2$  from below, the top-hat perturbation is only marginally bound and would collapse arbitrarily far into the future. Plots of  $\theta$  vs.  $z_{\text{coll}}$  for several different values of  $\lambda_0 = 1 - \Omega_0$  are shown in Fig. 1.

The virial temperature and velocity dispersion in this SUS approximation are derived as follows. The kinetic energy in the virialized state is

$$K = E - W_{\text{tot}} = \frac{3}{5} \frac{GM_0^2}{r_m} [1 + \theta(1 - 3\eta^2)]. \quad (22)$$

This kinetic energy is the energy of random internal motions only ( $T_{\text{kin}} = 0$ ). To obtain the equivalent temperature, we express the thermal energy as

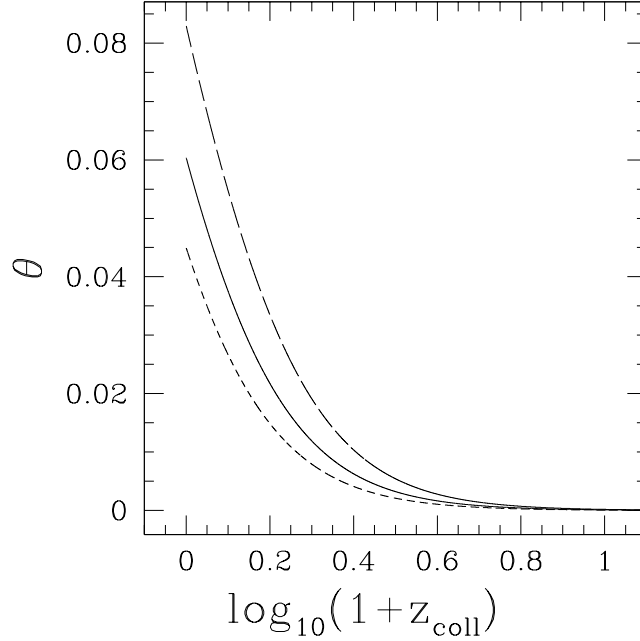


**Figure 1.** Dimensionless parameter  $\theta = \rho_\lambda/\rho_m$ , the ratio of the cosmological constant energy density to matter rest-mass energy density inside the top-hat at maximum expansion, versus the collapse redshift of the top-hat,  $z_{\text{coll}}$ , for different flat background universes, as labeled with the values of  $\lambda_0$ :  $\lambda_0 = 0.6$  (short-dashed line),  $\lambda_0 = 0.7$  (solid curve), and  $\lambda_0 = 0.8$  (long-dashed line).

$$U_{\text{th}} = \frac{3}{2} \frac{k_B T}{m} M_0, \quad (23)$$

where  $m$  is the mean mass per gas particle. If  $m_H$  is the mass of a hydrogen atom, then  $m = \mu m_H$ , where  $\mu$  is the mean molecular weight. The virial temperature is, therefore, given by equations (22) and (23) as

$$T = \frac{2}{5} \frac{G M_0 m}{k_B r_m} [1 + \theta(1 - 3\eta^2)]. \quad (24)$$

This temperature is always higher than the corresponding temperature with no cosmological constant. The maximum departure from the case with  $\Lambda = 0$  is 30%, for  $\theta = 1/2$ , for which  $\eta = 0.366$ . Henceforth, we shall refer to the virial temperature in equation (24) as  $T_{\text{SUS}}$ . For the case of a collisionless gas, we replace the virial temperature above by the virial velocity dispersion,

$$\sigma_V^2 = \frac{\langle v^2 \rangle}{3} = \frac{k_B T}{m}. \quad (25)$$

For a given  $\theta$ , the mean overdensity of the virialized object in the SUS approximation with respect to the critical density of the universe at  $z_{\text{coll}}$  is

$$\Delta_c \equiv \frac{\bar{\rho}}{\rho_{\text{crit}}(z_{\text{coll}})} = \frac{\Omega_0 a_0^3}{\theta \eta^3(\theta)} \left[ \frac{\rho_{\text{crit}}(z_{\text{coll}})}{\rho_{\text{crit},0}} \right]^{-1}, \quad (26)$$

where  $a_0$  is defined by equation (7), according to which  $\Omega_0 a_0^3 = \lambda_0$  if  $\Omega_0 + \lambda_0 = 1$ , and where equations (5) and (6) yield

$$\frac{\rho_{\text{crit}}(z_{\text{coll}})}{\rho_{\text{crit},0}} = \left[ \frac{h(z_{\text{coll}})}{h} \right]^2 = (1 - \Omega_0 - \lambda_0)(1 + z_{\text{coll}})^2 + \Omega_0(1 + z_{\text{coll}})^3 + \lambda_0. \quad (27)$$

Equations (20), (26) and (27) form a set of simultaneous equations which may be solved for the dependence of  $\eta$  and  $\theta$  on  $z_{\text{coll}}$ , once  $\Delta_c$  is known by integrating the nonlinear top-hat perturbation differential equation (10) [or (13)]. In general, this solution for the dependence of  $\eta$  and  $\theta$  on  $z_{\text{coll}}$  for a given  $\Delta_c$  involves the roots of a cubic equation which can be cumbersome to express analytically. However, for  $\theta \ll 1$  ( $z_{\text{coll}} \gg 1$ ), a good approximate solution is given by

$$\eta = 2q + \frac{1}{2}, \quad (28)$$

and

$$\theta = \frac{q}{\eta^3}, \quad (29)$$

where

$$q \equiv \frac{\Omega_0 a_0^3}{\Delta_c} \left[ \frac{h(z_{\text{coll}})}{h} \right]^{-2}. \quad (30)$$

The dependence of the quantity  $\Delta_c$  on  $z_{\text{coll}}$  can be expressed in terms of approximate analytical fitting formulae (with errors  $\sim 1\%$ ) according to

$$\Delta_c = 18\pi^2 + c_1 x - c_2 x^2, \quad (31)$$

where  $x \equiv \Omega(z_{\text{coll}}) - 1$ , and  $c_1 = 82$  (60) and  $c_2 = 39$  (32) for the flat (open) cases,  $\Omega_0 + \lambda_0 = 1$  ( $\Omega_0 < 1, \lambda_0 = 0$ ), respectively (Bryan & Norman 1998), where

$$\Omega(z) = \frac{\Omega_0(1+z)^3}{(1 - \Omega_0 - \lambda_0)(1+z)^2 + \Omega_0(1+z)^3 + \lambda_0}. \quad (32)$$

Henceforth, we shall refer to the quantities  $\eta$  and  $\Delta_c$  for the SUS approximation as  $\eta_{\text{SUS}}$  and  $\Delta_{c,\text{SUS}}$ .

### 3 ISOTHERMAL SPHERES IN THE PRESENCE OF THE X-COMPONENT

For matter-dominated universes, both open and flat, the final virialized object decouples from the expanding cosmological background from which it condensed. Hence, when we

describe it as an isothermal sphere in hydrostatic equilibrium, we do so in the usual non-cosmological way (e.g. Binney and Tremaine 1987). Similarly, in the presence of an X-component, the final virialized object also decouples from the expanding cosmological background from which it condensed, but it continues to be affected by the X-component because of the modification that component causes to the gravity force, as discussed earlier. We can still describe it as an isothermal sphere in hydrostatic equilibrium in the usual non-cosmological way, but we must account properly for this modification of the gravity force. The Poisson equation in equation (8) for the gravitational potential in the case of spherical symmetry is

$$\frac{1}{r^2} \frac{d}{dr} \left( r^2 \frac{d\Phi_{\text{tot}}}{dr} \right) = -4\pi G(\rho + \rho_{\text{X,eff}}). \quad (33)$$

The equation of hydrostatic equilibrium,  $\nabla p = \rho \mathbf{g}$ , where  $g = -\nabla \Phi_{\text{tot}}$ , combines with equation (33) in spherical symmetry to become

$$\frac{k_B T}{m} \frac{d\rho}{dr} = -\rho \nabla \Phi_{\text{tot}} = -\rho \frac{GM(r)}{r^2} - \rho \frac{4\pi G r \rho_{\text{X,eff}}}{3}, \quad (34)$$

where  $M(r)$  is the mass inside radius  $r$ . Multiplying equation (34) by  $r^2 m / \rho k_B T$  and taking the derivative with respect to  $r$ , we obtain

$$\frac{d}{dr} \left( r^2 \frac{d(\ln \rho)}{dr} \right) = -4\pi \frac{Gm}{k_B T} (\rho + \rho_{\text{X,eff}}) r^2. \quad (35)$$

Let us consider the case of collisionless particles, too. The equilibrium velocity distribution of the particles is a Maxwellian distribution given by

$$f(v) = \frac{\rho_0}{(2\pi\sigma_V^2)^{3/2}} \exp \left( -\frac{\Phi_{\text{tot}} - v^2/2}{\sigma_V^2} \right), \quad (36)$$

where  $\rho_0$  is the central density if we take  $\Phi_{\text{tot}}(r=0) = 0$ , and  $\sigma_V$  is the one-dimensional velocity dispersion. After integrating over velocity, we obtain

$$\rho = \int f(v) d\mathbf{v} = \rho_0 e^{\Phi_{\text{tot}}/\sigma_V^2}, \quad (37)$$

which we substitute into equation (33), to obtain

$$\frac{d}{dr} \left( r^2 \frac{d(\ln \rho)}{dr} \right) = -\frac{4\pi}{\sigma_V^2} G(\rho + \rho_{\text{X,eff}}) r^2. \quad (38)$$

By calculating the mean square velocity we obtain

$$\langle v^2 \rangle = 3\sigma_V^2. \quad (39)$$

The equivalent temperature can be calculated from

$$\frac{\langle v^2 \rangle}{2} = \frac{3 k_B T}{2 m} \quad (40)$$

to obtain for  $\sigma_V$ :

$$\sigma_V^2 = \frac{k_B T}{m}. \quad (41)$$

A comparison of equation (38) with equation (35) using equation (41) shows they are identical. Hence, the structure of a self-gravitating isothermal fluid sphere in hydrostatic equilibrium for  $\gamma = 5/3$  is identical with that for a spherically-symmetric system of collisionless particles in virial equilibrium with three-dimensional particle orbits which are isotropic and have a spatially uniform velocity dispersion.

To make equation (38) nondimensional, we introduce new variables

$$\tilde{\rho} = \frac{\rho}{\rho_0}, \quad \zeta = \frac{r}{r_0}, \quad \tilde{\rho}_{X,\text{eff}} = \frac{\rho_{X,\text{eff}}}{\rho_0}, \quad (42)$$

where  $\rho_0$  is the central density, and we choose

$$r_0 = \sigma_V / (4\pi G \rho_0)^{1/2}. \quad (43)$$

In terms of these variables, equation (38) becomes

$$\frac{d}{d\zeta} \left( \zeta^2 \frac{d(\ln \tilde{\rho})}{d\zeta} \right) = -\zeta^2 (\tilde{\rho} + \tilde{\rho}_{X,\text{eff}}). \quad (44)$$

We must solve equation (44) with the following boundary conditions:

$$\tilde{\rho}(0) = 1, \quad \frac{d\tilde{\rho}}{d\zeta}(0) = 0. \quad (45)$$

An important difference between equation (44) and the standard isothermal Lane-Emden equation should be noted here. The standard form of the equation for the case without the X-component does not provide a natural cutoff of the density profile, and, thus, both the profile and the mass are infinite. In the presence of an X-component, however, the modified Lane-Emden equation shows that the density profile is finite as long as  $n < 2$ , since there is a matter density below which the matter cannot be gravitationally bound. According to equation (44), this cutoff occurs at  $\rho(r) = -\rho_{X,\text{eff}}$ . For the special case of a cosmological constant, this cutoff occurs where  $\rho = 2\rho_\lambda$ . The mass of any such halo is, therefore, also finite and depends on the value of  $\rho_{X,\text{eff}}$ .

In Figure 2, we specialize to the cosmological constant case and plot the dimensionless density profile  $\rho/\rho_0$ , the logarithmic slope of this density profile, and the dimensionless circular velocity profile  $v_c/\sigma_V$ , normalized to the velocity dispersion  $\sigma_V$ , all as functions of

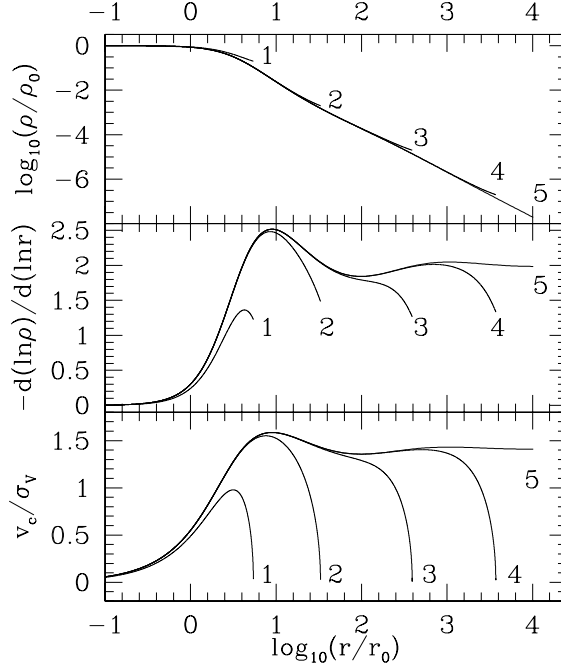


**Figure 2.** Modified Isothermal Lane-Emden Spheres in the Presence of a Cosmological Constant. (top panel) Density profile (in units of the central density  $\rho_0$ ) versus radius (in units of the core radius  $r_0$ ) when the X-component is a cosmological constant, for  $\tilde{\rho}_\lambda = 0.1$  (label 1),  $\tilde{\rho}_\lambda = 0.001$  (label 2),  $\tilde{\rho}_\lambda = 10^{-5}$  (label 3),  $\tilde{\rho}_\lambda = 10^{-7}$  (label 4), and  $\tilde{\rho}_\lambda = 0$  (no cosmological constant; label 5). Each plot extends out to its natural cutoff at  $\rho = 2\rho_\lambda$ , except the matter-dominated one (curve 5), which is infinite and is plotted only out to  $r/r_0 = 10^4$ . (middle panel) The logarithmic slopes of these density profiles versus dimensionless radius. (bottom panel) The circular velocity profiles  $v_c$  (normalized by the velocity dispersion of the halo  $\sigma_V$ ) versus dimensionless radius. Note the steep fall of the circular velocity close to the cutoff radius due to the fact that outer shells are only marginally bound in the presence of cosmological constant, unlike the case  $\Lambda = 0$ .

$r/r_0$  for several representative values of  $\tilde{\rho}_\lambda$ . In the presence of a cosmological constant, this circular velocity is:

$$v_c^2(r) \equiv r \frac{d\Phi}{dr} = \frac{GM(r)}{r} \left( 1 - 2 \frac{\rho_\lambda}{\rho(r)} \right). \quad (46)$$

When  $\rho_{X,\text{eff}} = 0$ , there is a well-known, analytical, power-law solution to the isothermal Lane-Emden equation, if we relax the inner boundary conditions in equation (45) so as to permit a singularity at the origin. This singular isothermal sphere (SIS) solution is given by

$$\rho(r) = \frac{\sigma_V^2}{2\pi G r^2}, \quad (47)$$

and

$$\sigma_V^2 = \frac{1}{2} \frac{GM(r)}{r} = \text{constant}. \quad (48)$$

For the modified isothermal Lane-Emden equation in the presence of the X-component, however, no such analytical solution is possible. Nevertheless, since  $\rho(r) \ll \rho_\lambda$  over most of the profile, except for the outer parts, the SIS solution is still a reasonable approximate solution of equation (44) out to  $\rho \sim \rho_\lambda$ . As for the case  $\rho_{X,\text{eff}} = 0$ , this approximate SIS



solution when  $\rho_{X,\text{eff}} \neq 0$  also does not satisfy the inner boundary condition in equations (45). We will compare our results for the nonsingular case with this approximate SIS solution in § 6.1 below, after we complete our derivation of the nonsingular TIS solution.

As mentioned above, unlike the standard result when  $\rho_{X,\text{eff}} = 0$ , isothermal spheres in the presence of the X-component always have a finite radius and mass. Hence, unlike the case with no X-component, we do not need to truncate these spheres in order to apply them to describe realistic finite structures. However, as will be shown below, our final TIS model actually imposes a smaller truncation radius  $r_t$  than that which corresponds to the marginally bound mass shell in the isothermal sphere solution. The total mass  $M_0$  of the isothermal sphere is then

$$M_0 = M(r_t) = \int_0^{r_t} 4\pi\rho(r)r^2 dr = 4\pi\rho_0 r_0^3 \tilde{M}(\zeta_t), \quad (49)$$

where  $\zeta_t = r_t/r_0$  and  $\tilde{M}(\zeta_t)$  is the dimensionless mass:

$$\tilde{M}(\zeta_t) \equiv \frac{M(r_t)}{4\pi r_0^3 \rho_0} = \int_0^{\zeta_t} \tilde{\rho}(\zeta) \zeta^2 d\zeta. \quad (50)$$

If such a truncation radius  $r_t$  does exist, this leads to the necessity of an external pressure to keep the system in equilibrium, which requires the inclusion of a surface pressure term in the virial theorem. This correction and its consequences are discussed in the next section.

#### 4 THE VIRIAL THEOREM FOR TRUNCATED ISOTHERMAL SPHERES IN A LOW DENSITY UNIVERSE

Let us consider the general isothermal sphere density profile,  $\rho(r)$ , obtained in the previous section. From the ideal gas law, the pressure inside the sphere as a function of the radius is

$$p(r) = \frac{k_B T}{m} \rho(r) = \sigma_V^2 \rho(r), \quad (51)$$

and at the outer edge

$$p_t = p(r_t) = \sigma_V^2 \rho(r_t). \quad (52)$$

The mean pressure inside the sphere is

$$\bar{p} = \frac{\int p dV}{\int dV} = \frac{3 \int_0^{\zeta_t} \tilde{\rho}(\zeta) \zeta^2 d\zeta}{\zeta_t^3 \tilde{\rho}(\zeta_t)} p_t = \frac{3\tilde{M}(\zeta_t)}{\zeta_t^3 \tilde{\rho}(\zeta_t)} p_t \equiv \alpha(\zeta_t) p_t, \quad (53)$$

where  $\zeta_t \equiv r_t/r_0$ .

The virial theorem for a static sphere in the presence of a surface pressure and of the X-component now becomes

$$3(\gamma - 1)K + W + S_p - 2W_X = 0, \quad (54)$$

where  $K$  is once again just  $U_{th}$ , and  $S_p$  is the surface pressure term. The thermal energy for a gas with a ratio of specific heats  $\gamma = 5/3$  is given by

$$U_{th} = \frac{1}{\gamma - 1} \int p dV = \frac{\alpha(\zeta_t)p_t V}{\gamma - 1} = \frac{3}{2}\alpha p_t V, \quad (55)$$

where  $V$  is the total volume. The surface term is equal to

$$S_p = - \int p \mathbf{r} \cdot d\mathbf{S} = -3V p_t. \quad (56)$$

Hence, according to the virial theorem, the unmodified gravitational potential energy term  $W$  is

$$W = -2\frac{\alpha - 1}{\alpha}U_{th} + 2W_X, \quad (57)$$

and the total energy is

$$E = \frac{2 - \alpha}{\alpha}U_{th} + 3W_X. \quad (58)$$

In order for the halo to be bound, the condition  $E < 0$  must be met, which requires

$$\alpha > \frac{2}{1 - 3\frac{W_X}{U_{th}}}. \quad (59)$$

The virial temperature of this generalized isothermal sphere is

$$T = \frac{2\alpha}{5(\alpha - 2)} \frac{GM_0 m}{k_B r_m} [1 + \theta(1 - 3\eta^2)], \quad (60)$$

which we shall henceforth refer to as  $T_{TIS}^*$ .

For  $\theta = 0$ , the temperature in equation (60) reduces to  $T_{TIS}$  derived in Paper I. In the presence of the X-component, this temperature is always slightly higher than the corresponding temperature for  $\rho_X = 0$ , however, but never by more than 5%, with the maximum reached for  $\theta = 0.5$ . Since  $\alpha/(\alpha - 2) > 1$  for any  $\alpha$ , the temperature  $T_{TIS}$  is always higher than  $T_{SUS}$ , the standard value for a uniform sphere shown in equation (24).

Just as we did in Paper I, we identify the virial radius  $r_{vir}$  with the size of the truncated isothermal sphere (i.e.  $r_{vir} = r_t$ ). For comparisons with the results of dynamical calculations

\* Henceforth, as in Paper I, the notation “TIS” shall refer to a solution of the isothermal Lane-Emden equation (modified here to account for the presence of the X-component), with the nonsingular boundary conditions of equation (45) at the origin.

of the formation of such an equilibrium object, we should interpret  $r_{\text{vir}}$  (and  $r_t$ ) as the radius inside which hydrostatic equilibrium holds (e.g. Cole & Lacey 1996). Hereafter, we specialize the discussion to the case in which the X-component is the cosmological constant.

## 5 CHOOSING A UNIQUE PROFILE: THE MINIMUM-ENERGY SOLUTION IN A LOW-DENSITY UNIVERSE

### 5.1 The Nonsingular, Truncated Isothermal Sphere Formed by Top-Hat Collapse

The virialized object which results from the collapse of a given top-hat density perturbation must have the mass of the top-hat before it collapsed and virialized. We assume that the total energy  $E$  is also conserved, including the effect the cosmological constant has on the potential energy, if present. Fixing the mass  $M_0$  and the energy  $E$  of the TIS which results from the collapse of the top-hat, however, is not enough to specify which member of the infinite family of solutions of the modified isothermal Lane-Emden equation which all share this mass and energy is chosen by the collapsing top-hat. In order to make a unique choice, some additional information is required, such as the value of the boundary pressure  $p_t$ . As in Paper I, we shall assume that the correct boundary pressure  $p_t$  is that value which makes the TIS with this total energy  $E$  and mass  $M_0$  correspond to the unique minimum-energy solution. In order to determine the minimum-energy TIS which results from a given top-hat collapse, we must take account of the fact that this top-hat collapse depends upon the value of the parameter  $\theta$ . This parameter measures the relative importance of the vacuum energy density associated with the cosmological constant and the rest-mass energy density of the matter inside the top-hat at maximum expansion, which is different for different epochs of maximum expansion even for a given value of the cosmological constant. As a result, the internal structure of the TIS solution which results from a given top-hat collapse even when expressed in dimensionless form with radius in units of  $r_0$  and density in units of  $\rho_0$  will depend, not only upon the background cosmology parameters (i.e.  $\Omega_0 = 1 - \lambda_0$  and  $H_0$ ), but also upon  $z_{\text{coll}}$  for the top-hat. This makes the calculation of our minimum-energy TIS solution in this case more complicated than for the EdS case in Paper I.

As in Paper I, this conservation of the energy  $E$  of the top-hat before and after its collapse

and virialization assumes that there is no extra  $pdV$ -work that needs to be taken into account due to the presence of the external boundary pressure  $p_t$  which would otherwise alter the final total energy  $E$  compared with its initial value before collapse. This is appropriate for the case at hand, since the collapse prior to the epoch of virialization is that of a cold, pressure-free gas which collapses supersonically. As in the well-known, self-similar, spherical infall solution of Bertschinger (1985), the original energy is converted from potential energy at maximum expansion to a mixture of infall kinetic energy and potential energy during infall, with a negligible share of the energy going into compressional heating. In that solution, the infall is halted by a strong shock. At this shock, the kinetic energy of infall is converted primarily into the thermal energy of the shock-compressed gas, with only a small portion remaining as kinetic energy of subsonic, postshock infall. While the self-similar infall solution is strictly correct only for the EdS universe, we expect similar behaviour in low density universes, as well. However, since no general self-similar infall solution exists in these cases, the analogous infall solution for low-density universes must be studied by numerical means. Of course, in the limit of high redshift, the self-similar solution of the EdS case can be applied even to the case of a low-density universe if properly rescaled (see Appendix A).

By analogy with this infall solution, therefore, we identify the boundary pressure  $p_t$  in the case of our TIS solution, not as a fixed external pressure which acts on the top-hat boundary throughout its collapse and virialization, but rather as something like the instantaneous post-shock pressure in the infall solution. As such, it has a physical origin in the conversion of the original energy of the collapsing top-hat, itself, from potential energy at maximum expansion into kinetic energy of infall during collapse and, finally, into thermal energy of the post-shock gas, always conserving the original energy  $E$  of the top-hat.

## 5.2 Finding the Unique Minimum-Energy Solution

### 5.2.1 Flat Universe with Cosmological Constant

As shown above, the truncated isothermal sphere solutions form a one-parameter family, described by  $\zeta_t = r_t/r_0$  – the truncation radius in units of the core radius. Specifying  $\zeta_t$ , the total mass, and the total energy completely determines the solution. Alternatively, we can specify the mass, the total energy and the applied external pressure  $p_t$ .

The conservation of energy equates the energy after collapse and virialization to the energy of the top-hat at maximum expansion,  $E(t_m) = E_{\text{vir}}$ . This yields

$$-\frac{3}{5} \frac{GM_0^2}{r_m} \left(1 + \frac{\rho_\lambda}{\rho_m}\right) = \frac{2-\alpha}{\alpha} U_{\text{th}} M_0 - 16\pi^2 G \rho_\lambda I_t, \quad (61)$$

where

$$I_t \equiv \int_0^{r_t} \rho r^4 dr. \quad (62)$$

In dimensionless variables, equation (61) becomes

$$(1 + \theta) \eta_{\text{TIS}} = \frac{5}{2} \frac{\alpha - 2}{\alpha} \frac{\zeta_t}{\tilde{M}_t} + \frac{5\theta \eta_{\text{TIS}}^3 \tilde{I}_t}{\tilde{M}_t \zeta_t^2}, \quad (63)$$

where

$$\tilde{I}_t \equiv \int_0^{\zeta_t} \tilde{\rho} \zeta^4 d\zeta, \quad (64)$$

and we have used the fact that

$$\tilde{\rho}_\lambda = \frac{\rho_\lambda}{\rho_0} = \frac{\rho_\lambda}{\rho_m} \frac{\rho_m}{\rho_0} = \frac{3\theta \eta_{\text{TIS}}^3 \tilde{M}_t}{\zeta_t^3}. \quad (65)$$

For a given external pressure  $p_t$ , the total energy of the modified isothermal Lane-Emden sphere is given by

$$\begin{aligned} E &= -\frac{3}{5} \frac{GM_0^2}{r_m} (1 + \theta) = -\frac{3}{5} \frac{GM_0^2}{r_0} (1 + \theta) \frac{\eta_{\text{TIS}}}{\zeta_t} \\ &= \frac{3}{5} (4\pi^3 G)^{1/4} M_0^{3/2} p_t^{1/4} (1 + \theta) \tilde{E}(\zeta_t), \end{aligned} \quad (66)$$

where

$$\tilde{E}(\zeta_t) = -\frac{\eta_{\text{TIS}} \tilde{M}_t^{1/2}}{\zeta_t \tilde{\rho}_t^{1/4}}. \quad (67)$$

We have plotted the dependence of the dimensionless total energy  $\tilde{E}$  on  $\zeta_t$  in Figure 3 for several representative values of the parameter  $\theta$ . In order to indicate the dependence of the size of the sphere on  $\zeta_t$ , we can nondimensionalize the radius  $r_t$ , according to

$$-\lambda_E \equiv -\frac{r_t E}{GM_0^2} = \frac{3}{5} (1 + \theta) \eta_{\text{TIS}}. \quad (68)$$

This definition of  $\lambda_E$  also corresponds to the familiar dimensionless energy parameter used in discussions of the stability of isothermal spheres.

For a given mass  $M_0$  and external pressure  $p_t$ , the solution is specified uniquely only if we can uniquely identify a special value of  $\zeta_t$ , or equivalently, of  $E$ . Apparently, for any truncated isothermal sphere of mass  $M_0$  which is confined by a given external pressure  $p_t$ ,

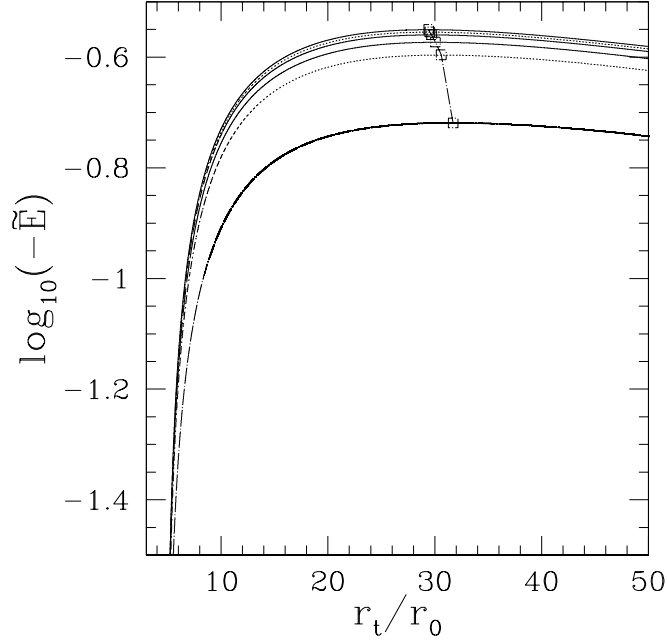


**Figure 3.** The dimensionless energy  $\tilde{E}(\zeta_t)$  versus dimensionless truncation radius  $\zeta_t = r_t/r_0$  for several representative values of  $\theta$  (see also Table 1), chosen as described in §5.3. From top to bottom:  $\theta = 0$  (matter-dominated models),  $\theta = 0.0118$ ,  $\theta = 0.0249$ ,  $\theta = 0.0604$ ,  $\theta = 0.123$ , and  $\theta = 0.5$ . The symbols indicate the minimum-energy points for each curve.

there is a unique value of  $\zeta_t$  which minimizes the total energy  $E$ . As in Paper I, we shall make the reasonable ansatz that this minimum-energy solution is the unique TIS solution preferred in nature as the outcome of the virialization of the sphere in the presence of a fixed external pressure. We offered evidence to support this ansatz in Paper I. It is possible that this is a general result for any TIS formed by relaxation in the presence of a fixed external pressure, but we are only concerned here with spheres that evolve from cosmological initial conditions.

For each value of  $\theta$  in the allowed range  $0 \leq \theta \leq 0.5$ , the minimum value of  $E$  as a function of  $\zeta_t$  for a given  $p_t$  is found by minimizing the dimensionless energy  $\tilde{E}(\zeta_t)$  in equation (67), with  $\eta_{\text{TIS}}$  found by solving equation (63). Unlike the EdS case discussed in Paper I, the minimum-energy solution in a low-density universe is not universal (except for the special case  $\Lambda = 0$ ), but instead depends upon the time of collapse, as implicitly parameterized by the quantity  $\theta$ . This makes our calculation of the solution more complicated than in Paper I, since equation (44) depends upon  $\tilde{\rho}_\lambda$  and must, therefore, be solved in conjunction with equation (65) to obtain a self-consistent solution and, subsequently, to find the minimum-energy point. As can be seen in Figure 3, the minimum of the energy

corresponds in each curve to a unique value of the dimensionless truncation radius  $\zeta_t$  and becomes more pronounced when the cosmological constant contribution is more important. The value of  $\zeta_t$  at which this minimum energy occurs increases with increasing  $\tilde{\rho}_\lambda$ , from  $\zeta_t = 29.4$  for matter-dominated models ( $\theta = 0$ ) to  $\zeta_t = 31.7$  for  $\theta = 0.5$ , the maximum allowed value. The resulting values for  $\zeta_t$ ,  $\alpha(\zeta_t)$ ,  $\eta_{\text{TIS}}$ ,  $R \equiv \rho_0/\rho_t$ ,  $\tilde{\rho}_\lambda$ , and  $\tilde{M}_t$  versus  $\theta$  are shown in Figure 4. The point  $\theta = 0$  corresponds to the solution for matter-dominated models without cosmological constant (either open or flat), where these dimensionless quantities are identical to those for the EdS case obtained in Paper I.

Thus far, we have derived the unique, dimensionless minimum-energy TIS solution for the postcollapse virialized object which results from top-hat collapse at any epoch for different cosmologies, as parameterized by the value of  $\theta = \rho_\lambda/\rho_m$ , the ratio of the vacuum energy density to the matter rest-mass energy density of the top-hat at its epoch of maximum expansion. In order to complete the dimensionless description of the TIS model for the postcollapse equilibrium object created by a top-hat which collapses at a given redshift  $z_{\text{coll}}$ , it is necessary to relate  $\theta$  to  $z_{\text{coll}}$ , according to the solution of the nonlinear top-hat perturbation equation (10) [or (13)]. This dependence of  $\theta$  on  $z_{\text{coll}}$  for the top-hat perturbation was described in § 2 above.

The parameters we have derived for the unique minimum-energy TIS solution for several representative values of the parameter  $\theta$ , chosen so as to span the allowed range, are summarized in Table 1. These values of the parameter  $\theta$  were chosen to correspond to the EdS case and open-matter-dominated cases ( $\theta = 0$ ), and to the flat,  $\Lambda$ -dominated model currently favoured by astronomical observations, with  $\lambda_0 = 0.7$ , for different collapse epochs:  $z_{\text{coll}} = 1$  ( $\theta = 0.01183$ ),  $z_{\text{coll}} = 0.5$  ( $\theta = 0.0249$ ), and  $z_{\text{coll}} = 0$  ( $\theta = 0.0604$ ), as well as for the extreme cases of  $\lambda_0 = 0.9$ ,  $z_{\text{coll}} = 0$  ( $\theta = 0.123$ ), and of either  $\lambda_0 \rightarrow 1$  or else  $1 + z_{\text{coll}} \rightarrow 0$  (i.e. in the future) ( $\theta = 0.5$ ). If we adopt  $\lambda_0 \leq 0.9$  as a reasonably conservative estimate of the possible range allowed by astronomical observation, then the maximum value of  $\theta$  of interest corresponds to that for which  $z_{\text{coll}} = 0$ , i.e.  $\theta(\lambda_0 = 0.9, z_{\text{coll}} = 0) = 0.123$ .

The radius  $r_t$  of the TIS solution is encountered by the outer boundary of the collapsing top-hat at a time somewhat earlier than the time  $t_{\text{coll}}$  of infinite density in the top-hat solution. We shall refer to the time at which the radius of the collapsing top-hat equals  $r_t$  as  $t_{\text{cross}}$ , to distinguish it from  $t_{\text{coll}}$ . At time  $t_{\text{cross}}$ , the top-hat exact solution yields an

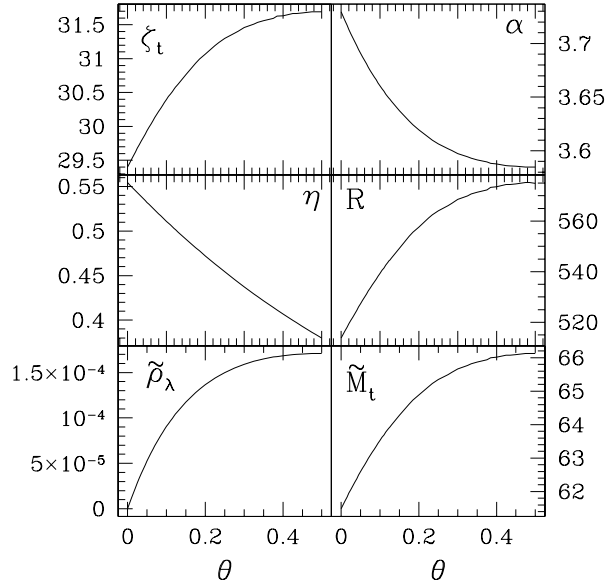


**Figure 4.** Dimensionless parameters of the TIS model in a flat universe with cosmological constant vs. the parameter  $\theta$ , where  $\theta \equiv \rho_\lambda/\rho_m$ , the ratio of the vacuum energy density to the matter rest-mass energy density at maximum expansion of the parent top-hat.

overdensity  $\delta = \delta_{\text{cross}} \approx 100$  for EdS universe, while the extrapolated linear solution at this time yields  $\delta_{L,\text{cross}} \approx 1.56$ . For a flat, low-density universe, however, both  $\delta_{\text{cross}}$  and  $\delta_{L,\text{cross}}$  exceed their values for the EdS case. For example, if  $z_{\text{coll}} = 0$ , then  $\delta_{\text{cross}} = 197(416)$  and  $\delta_{L,\text{cross}} = 1.96(2.52)$  for  $\lambda_0 = 1 - \Omega_0 = 0.7(0.9)$ , respectively. For  $\lambda_0 \rightarrow 1$  or else in the future for any value of  $\lambda_0$ , both  $\delta_{\text{cross}} \rightarrow \infty$  and  $\delta_{L,\text{cross}} \rightarrow \infty$ . If we assume that the TIS forms instantaneously at  $t = t_{\text{cross}}$ , then its mean density corresponds to a mean overdensity  $\bar{\delta} = \delta_{\text{cross}}$  when compared with the background density at  $z_{\text{cross}}$ , but the same TIS corresponds to a mean overdensity  $\bar{\delta} = \delta_{\text{coll}}$ , which is larger than this  $\delta_{\text{cross}}$  by about 30%, when compared with the background density at  $z_{\text{coll}}$ . This value of  $\delta_{\text{coll}}$  differs somewhat from the conventional value of  $\bar{\delta}(t_{\text{coll}})$  found for the postcollapse virialized sphere in the SUS approximation. The values of  $\delta_{\text{cross}}$ ,  $\delta_{L,\text{cross}}$ , and  $\delta_{\text{coll}}$  for our chosen set of illustrative values of  $\theta$  are also given in Table 1.

As noted in Paper I, applications of the top-hat model involving the Press-Schechter approximation customarily identify the characteristic time of formation of objects of a given mass as the finite time at which the nonlinear perturbation solution predicts collapse to infinite density, at which time the linear solution yields  $\delta_L = \delta_{\text{crit}}$ . Since  $\delta_{L,\text{cross}} < \delta_{\text{crit}}$ ,



it may be appropriate to replace  $\delta_{\text{crit}}$  in such applications by the value  $\delta_{L,\text{cross}}$ , implying that the number of objects formed at any epoch with a mass greater than some value may be somewhat higher for the TIS solution than previously assumed in applications of the Press-Schechter approximation.

### 5.2.2 Open, Matter-Dominated Universe: Low-Density Universe without X-component

For a matter-dominated universe,  $\theta = 0$ , and the family of solutions obtained in § 5.2.1 reduces to a single dimensionless solution, which is independent of  $\Omega_0$ , identical to the solution we obtained in Paper I. The dimensional solution, however, depends upon the background cosmology. The details of this dependence will be discussed in § 5.3. As for the case of the flat, low-density universe discussed above, both  $\delta_{\text{cross}}$  and  $\delta_{L,\text{cross}}$  for the low-density, matter-dominated case exceed their values for the EdS case. For example, if  $z_{\text{coll}} = 0$ , then  $\delta_{\text{cross}} = 222$  and  $\delta_{L,\text{cross}} = 3.29$  for  $\lambda_0 = 0, \Omega_0 = 0.3$ . As  $\Omega(z) \rightarrow 0$  (i.e. in the future), we again find that both  $\delta_{\text{cross}} \rightarrow \infty$  and  $\delta_{L,\text{cross}} \rightarrow \infty$ .

### 5.2.3 Stability

The TIS model in an EdS universe represents a stable solution of the isothermal Lane-Emden equation (Paper I). This conclusion holds for any matter-dominated model, as well. In the presence of an X-component, however, the Lane-Emden equation is modified, leading to a case whose stability, as far as we know, has not been studied. Nevertheless, since the TIS solution in the presence of the X-component departs from the solution for a matter-dominated universe by only a small amount for the observationally-constrained values of  $\lambda_0$ , we expect our solution for the low-density universe cases considered here to be stable, as well. However, detailed study of this problem is beyond the scope of this paper.

## 5.3 Dependence of the TIS Model Parameters on Halo Mass and Collapse Redshift for Different Background Cosmologies

In this section, we describe how the dimensional parameters for our dimensionless TIS solution are specified for a given mass  $M_0$  and collapse redshift  $z_{\text{coll}}$ . For a given  $\theta$ , the dimensionless minimum-energy TIS solution and the nonlinear top-hat perturbation solution

combine to yield the mean overdensity of the TIS solution with respect to the critical density of the universe at  $z_{\text{coll}}$ ,

$$\Delta_{\text{c,TIS}} \equiv \frac{\bar{\rho}}{\rho_{\text{crit}}(z_{\text{coll}})} = \frac{\Omega_0 a_0^3}{\theta \eta_{\text{TIS}}^3(\theta)} \left[ \frac{\rho_{\text{crit}}(z_{\text{coll}})}{\rho_{\text{crit},0}} \right]^{-1}, \quad (69)$$

(where  $\Omega_0 a_0^3 = \lambda_0$  for  $\Omega_0 + \lambda_0 = 1$ ). Note that this overdensity is somewhat different from the corresponding overdensity  $\Delta_{\text{c,SUS}}$  derived from the standard uniform sphere approximation as described in § 2.2, since the collapse factors  $\eta = r_m/r_t$  are different for the two cases. These two overdensities are simply related, however, as follows:

$$\Delta_{\text{c,TIS}} = \frac{\eta_{\text{SUS}}^3}{\eta_{\text{TIS}}^3} \Delta_{\text{c,SUS}}. \quad (70)$$

The dimensional parameters for the TIS solution for a given total halo mass  $M_0$  and  $\Delta_{\text{c,TIS}}$  can be expressed as follows:

$$r_t = \left( \frac{3M_0}{4\pi \Delta_{\text{c,TIS}} \rho_{\text{crit}}(z_{\text{coll}})} \right)^{1/3}, \quad (71)$$

$$r_m = \frac{r_t}{\eta_{\text{TIS}}} = \frac{\zeta_t}{\eta_{\text{TIS}}} r_0, \quad (72)$$

$$\rho_0 = \frac{\zeta_t^3}{3\tilde{M}_t} \bar{\rho} = \frac{\zeta_t^3}{3\tilde{M}_t} \Delta_{\text{c,TIS}} \rho_{\text{crit}}(z_{\text{coll}}), \quad (73)$$

$$\sigma_V^2 = 4\pi G \rho_0 r_0^2 = \left[ \frac{4\pi}{3} \Delta_{\text{c,TIS}} \rho_{\text{crit}}(z_{\text{coll}}) \right]^{1/3} \frac{\zeta_t}{\tilde{M}_t} G M_0^{2/3}, \quad (74)$$

$$T_{\text{TIS}} = \frac{m}{k_B} \sigma_V^2, \quad (75)$$

$$v_c(r) = \left[ \frac{GM(r)}{r} \left( 1 - 2 \frac{\rho_\lambda}{\rho(r)} \right) \right]^{1/2}. \quad (76)$$

For practical application of the TIS solution, we have provided a convenient set of accurate analytical fitting formulae for the dependences of the dimensionless parameters of the solution (e.g.  $\zeta_t$ ,  $\eta_{\text{TIS}}$ ,  $\tilde{M}_t$ ) on  $\theta$  in Appendix B. Since fitting formulae are also available for the dependence of  $\Delta_{\text{c,SUS}}$  on  $z_{\text{coll}}$  for different cosmological parameters ( $\lambda_0, \Omega_0$ ), in the form of equation (31), it is useful to express the dependence of  $\theta$  on  $z_{\text{coll}}$  for a given background cosmology by combining equations (26) and (27) to write

$$\theta = \frac{\Omega_0 a_0^3}{\Delta_{\text{c,SUS}} \eta_{\text{SUS}}^3} \left[ \frac{h(z_{\text{coll}})}{h} \right]^{-2}. \quad (77)$$

**Table 1.** Summary of the minimum-energy TIS solution in a flat universe with a cosmological constant for several illustrative values of  $\theta$ .

Quantity	$\theta = 0$	$\theta = 0.0118$	$\theta = 0.0249$	$\theta = 0.0604$	$\theta = 0.123$	$\theta = 0.5$
$\zeta_t = \frac{r_t}{r_0}$	29.400	29.534	29.677	30.04	30.58	31.69
$\alpha(\zeta_t) = \frac{\bar{p}}{p_t}$	3.730	3.720	3.709	3.684	3.649	3.585
$b_T = \frac{T_{TIS}}{T_{SUS}}$	2.156	2.163	2.170	2.188	2.213	2.262
$\tilde{M}(\zeta_t)$	61.48	61.76	62.06	62.80	63.90	66.13
$\tilde{\rho}_\lambda$	0	$1.405 \times 10^{-5}$	$2.842 \times 10^{-5}$	$6.166 \times 10^{-5}$	$1.042 \times 10^{-4}$	$1.710 \times 10^{-4}$
$\eta_{TIS} = \frac{r_t}{r_m}$	0.5544	0.5490	0.5432	0.5277	0.5016	0.3800
$\eta_{SUS}$	0.5	0.4970	0.4937	0.4845	0.4676	0.3660
$\frac{r_{t,TIS}}{r_{t,SUS}}$	1.109	1.105	1.100	1.089	1.073	1.038
$\delta_{L,cross}$	1.562 <sup>a</sup>	1.630	1.710	1.955	2.524	$\infty$
$\delta(t_{cross})$	102.6 <sup>a</sup>	116.2	133.5	196.8	416.1	$\infty$
$\delta_{TIS}(t_{coll})$	129.6	148.5	172.7	264.4	579.1	$\infty$
$\frac{\rho_t}{\rho_0}$	$1.946 \times 10^{-3}$	$1.934 \times 10^{-3}$	$1.920 \times 10^{-3}$	$1.887 \times 10^{-3}$	$1.837 \times 10^{-3}$	$1.739 \times 10^{-3}$
$\mathcal{R}$	514	517	521	530	544	575
$\frac{\rho_0}{\rho_{b,coll}}$	$1.796 \times 10^4$	$2.064 \times 10^4$	$2.430 \times 10^4$	$3.784 \times 10^4$	$8.641 \times 10^4$	$\infty$
$\frac{\rho_t}{\rho_{b,coll}}$	35.0	39.92	46.67	71.39	158.8	$\infty$
$\lambda_E$	-0.3326	-0.3333	-0.3340	-0.3357	-0.3380	-0.3420
$K/ W $	0.6832	0.6846	0.6861	0.6897	0.6948	0.7066

<sup>a</sup> These values are slightly different from the values quoted in Paper I, Table 1. The correct values are shown here. If we match the outer radius of this top-hat at its turnaround epoch to the radius of the mass shell in the self-similar infall solution of Bertschinger (1985) which contains the same mass at the same turnaround epoch, which we did in Paper I, that mass shell crosses the shock at  $\delta_L = 1.5572$ .

In that case, for a given  $z_{coll}$ ,  $\Omega_0$ ,  $\lambda_0$ , and  $h$ , equation (77) combines with equation (19) which relates  $\eta_{SUS}$  to  $\theta$  and the fitting formulae for  $\Delta_{c,SUS}$  as a function of  $z_{coll}$  in equation (31) to yield a pair of simultaneous algebraic equations for  $\theta$ .

For most cases of current interest (i.e.  $\Omega_0 \geq 0.3$ , which corresponds to  $\theta \leq 0.06$  for  $z_{coll} \geq 0$ ), a further approximation to these more accurate results is possible which is even simpler to use, if we neglect the effect of the cosmological constant on the dimensionless solution of the Lane-Emden equation. In particular, as long as we take proper account of the evolution of a top-hat density perturbation in a low-density universe up to its moment of infinite collapse and still satisfy energy conservation and the virial theorem, we will capture most of the dependence of the TIS solution on the background cosmology. The result can

be expressed as follows:

$$r_m = 337.7 \left( \frac{M_0}{10^{12} M_\odot} \right)^{1/3} [F(z_{\text{coll}})]^{-1} h^{-2/3} \text{ kpc}, \quad (78)$$

$$r_t = 187.2 \left( \frac{M_0}{10^{12} M_\odot} \right)^{1/3} [F(z_{\text{coll}})]^{-1} h^{-2/3} \text{ kpc}, \quad (79)$$

$$r_0 = 6.367 \left( \frac{M_0}{10^{12} M_\odot} \right)^{1/3} [F(z_{\text{coll}})]^{-1} h^{-2/3} \text{ kpc}, \quad (80)$$

$$T = 7.843 \times 10^5 \left( \frac{\mu}{0.59} \right) \left( \frac{M_0}{10^{12} M_\odot} \right)^{2/3} F(z_{\text{coll}}) h^{2/3} \text{ K}, \quad (81)$$

$$\sigma_V^2 = 1.098 \times 10^4 \left( \frac{M_0}{10^{12} M_\odot} \right)^{2/3} F(z_{\text{coll}}) h^{2/3} \text{ km}^2 \text{ s}^{-2}, \quad (82)$$

$$\rho_0 = 1.799 \times 10^4 [F(z_{\text{coll}})]^3 \rho_{b0} = 3.382 \times 10^{-25} [F(z_{\text{coll}})]^3 h^2 \text{ g/cm}^3. \quad (83)$$

where

$$F(z_{\text{coll}}) \equiv \left[ \frac{h(z_{\text{coll}})}{h} \right]^2 \frac{\Delta_{\text{c,TIS}}(z_{\text{coll}}, \lambda_0)}{\Delta_{\text{c,TIS}}(\lambda_0 = 0)} = \left[ \frac{\Omega_0}{\Omega(z_{\text{coll}})} \frac{\Delta_{\text{c,SUS}}}{18\pi^2} \right]^{1/3} (1 + z_{\text{coll}}). \quad (84)$$

For the EdS case,  $F = (1 + z_{\text{coll}})$ , while for an open, matter-dominated universe and a flat universe with a cosmological constant,  $F \rightarrow \Omega_0^{-1/3} (1 + z_{\text{coll}})$  at early times [i.e.  $x \rightarrow 0$ ]. Here  $\mu$  is the mean molecular weight, where  $\mu = 0.59$  (1.22) for an ionized (neutral) gas of H and He with  $[He]/[H] = 0.08$  by number. The relative accuracy of these formulae in comparison with the exact numerical results is plotted for the case  $\lambda_0 = 1 - \Omega_0 = 0.7$  in Figure 5, which shows that the errors are always small, even for  $z_{\text{coll}} = 0$ .

## 6 SUMMARY AND DISCUSSION

### 6.1 Comparison of the Minimum-Energy TIS Solution with the Standard Uniform Sphere and Singular Isothermal Sphere Approximations

The temperature derived here for the minimum-energy TIS solution for the postcollapse sphere in virial and hydrostatic equilibrium which follows top-hat collapse is a factor of approximately two larger than the value previously derived for the SUS approximation, i.e. by satisfying energy conservation and the virial theorem for a postcollapse sphere of uniform density for which the surface pressure term is neglected, as summarized in § 2. In particular, if we write  $T_{\text{TIS}} = b_T T_{\text{SUS}}$ , then  $b_T = \alpha/(\alpha - 2) \approx 2.2$ . The size of the TIS sphere, given in terms of the radius  $r_m$  of the top-hat at maximum expansion according to  $r_t = \eta_{\text{TIS}} r_m$ ,

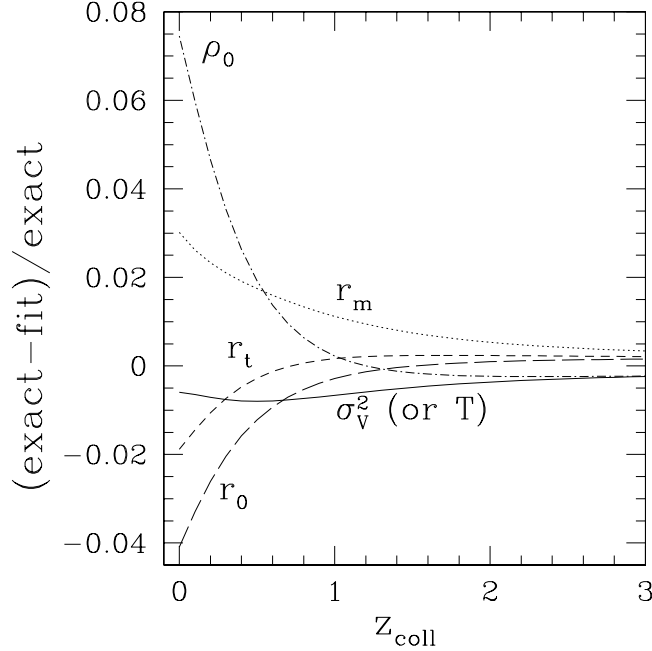


**Figure 5.** Fractional deviation of the approximate analytical fits in equations (78) – (83) from the exact numerical solution for background cosmology with  $\lambda_0 = 1 - \Omega_0 = 0.7$ , as labelled.

is actually not far from the size of the SUS sphere,  $r_{\text{vir}} = \eta_{\text{SUS}} r_m$ , as shown in Table 1. However, in terms of the TIS core radius  $r_0$  (where, recall, our  $r_{0,\text{TIS}} \equiv r_{\text{King}}/3$  as defined for conventional isothermal Lane-Emden spheres), the truncation radius is large,  $r_t/r_0 \geq 29.4$ , implying that the TIS is very far from uniform density. Despite this relatively small core radius, the TIS solution is also quite different from that of a *singular* isothermal sphere<sup>†</sup>. For the latter, the ratio of the average density to that at the surface is 3, while we find a value of 3.6 to 3.7 for the nonsingular TIS. The truncation radius in the singular limit is only  $r_t = (5/12)r_m$ , smaller than the radius of the TIS. Similarly, the correction factor for the virial temperature of this SIS relative to that of the SUS is  $b_T = 3$ , as opposed to the value for the TIS model which is  $b_T \approx 2$ . The central density of the TIS is  $> 1.8 \times 10^4$  times larger than the mean density of the background at the collapse epoch for the parent top-hat. Finally, the TIS solution predicts that the top-hat will virialize somewhat earlier than the nominal collapse time of the top-hat, since the outermost mass elements encounter a shock

<sup>†</sup> As discussed in § 3, the singular isothermal sphere is not an exact solution of the Lane-Emden equation in the presence of a cosmological constant, but for the purpose of this comparison, we ignore the effect of  $\Lambda \neq 0$  on this equation but take account of the more important effects of  $\Lambda \neq 0$  on the top-hat evolution, on the conservation of energy of the top-hat before and after its collapse and virialization and on the virial theorem.

**Table 2.** A comparison of three approximations for the postcollapse equilibrium structure of top-hat density perturbations in a low density universe.

	Uniform Sphere <sup>a</sup>	Singular Isothermal Sphere <sup>b</sup>	TIS Solution $\theta = 0 - 0.5^c$
$\eta/\eta_{\text{SUS}}$	1	0.833	1.11–1.04
$\frac{T}{T_{\text{SUS}}}$	1	3	2.16–2.26
$\frac{\rho_0}{\rho_t}$	1	$\infty$	514–575
$\frac{\langle \rho \rangle}{\rho_t}$	1	3	3.73–3.59
$\frac{r_t}{r_0}$	– NA –	$\infty$	29.4–31.7
$\frac{\Delta_c}{\Delta_{c,\text{SUS}}}$	1	$\left(\frac{6}{5}\right)^3 = 1.728$	1.36–1.12
$K/ W $	0.5	0.75	0.683–0.707

<sup>a</sup> A top-hat perturbation of a given mass collapses at a given redshift in a background universe with given values of  $\Omega_0$  and  $\lambda_0$ ; all of these values are held fixed in this comparison of the three approximations.

<sup>b</sup> These SIS numbers are an approximation which ignores the small modification of the Lane-Emden equation solution to take account of  $\Lambda \neq 0$ , but accounts for the more important effects of  $\Lambda \neq 0$  on top-hat evolution, energy conservation and the virial theorem.

<sup>c</sup> These values show the full range allowed for top-hat perturbations which collapse at finite time including the distant future (i.e.  $\lambda \rightarrow 1$ ).

and shell-crossings in the infall solution at finite radius. This implies that the standard value of  $\delta_{\text{crit}} \approx 1.69$  used in the Press-Schechter approximation for the halo mass function at a given time, based upon extrapolating the linear growth to the epoch at which the nonlinear top-hat solution predicts infinite density, should perhaps be replaced by  $(\delta_{\text{L,cross}})_{\text{TIS}} > 1.56$ . A comparison of the TIS model with the SUS and SIS approximations is summarized in Table 2.

## 6.2 Summary

We have generalized the TIS model, derived in Paper I for an Einstein-de Sitter universe, to the case of a low-density universe, either matter-dominated ( $\Omega_0 < 1, \lambda_0 = 0$ ) or flat with cosmological constant ( $\Omega_0 + \lambda_0 = 1$ ). The formalism we have presented can also be used to obtain the corresponding TIS solutions for other background cosmology models with a component of the energy density which remains homogeneous on scales relevant to the formation of virialized halos, such as quintessence. The halo density profile we have thus derived has a universal, time-invariant shape in the matter-dominated cases, when expressed in units of the central density  $\rho_0$  with radius in units of the core radius  $r_0$ . However, in the

presence of a cosmological constant, whose importance increases with time, the isothermal Lane-Emden equation is modified, and, as a result, this dimensionless TIS density profile is no longer time-invariant, but, instead, depends on the epoch of collapse. This dependence is relatively weak, except for the outer parts of the halo at late times. For example, for  $\lambda_0 = 0.7$  and  $z_{\text{coll}} = 0$ , the dimensionless radius of the halo  $r_t/r_0$  is 30.04, larger than the value of 29.40 for a matter-dominated universe by about 2% (see Table 1). At later times (i.e. in the future) in the  $\Lambda$ -dominated universe, however, the departure from the universal, time-invariant shape of the matter-dominated case will be more pronounced, with the dimensionless radius reaching 31.69, or  $\sim 8\%$  higher. For all low-density universe cases, including those which are matter-dominated, far more significant differences from the TIS model in an EdS universe, however, are found in the over-all amplitude of the density profile as measured relative to the mean density of the background. For example, the ratios of the average density inside the virial radius and of the central density to the cosmic mean background density at the epoch of collapse, are larger than their values for an EdS universe by more than a factor of 2, for the cases  $\Omega_0 = 0.3, \lambda_0 = 0$  and  $1 - \Omega_0 = \lambda_0 = 0.7$ , for halos which collapse today, while these ratios grow arbitrarily large in the future, due to the decrease of  $\Omega(t)$  with time in both cases.

The dimensional parameters of the TIS halo solution also depend significantly on the background cosmology. For example, a TIS halo of  $10^{10}h^{-1}M_\odot$  which collapses at  $z = 0$  in an EdS universe has a radius  $r_t = 40.35 h^{-1}\text{kpc}$ , central density  $\rho_0 = 3.38 \times 10^{-25} h^2 \text{g cm}^{-3}$ , and velocity dispersion  $\sigma_V = 22.6 \text{ km s}^{-1}$ , while a halo of the same mass which collapses at the same redshift, but in a flat universe with  $\lambda_0 = 0.7$ , is  $\sim 18\%$  larger, with a 33% lower central density, and  $\sim 9\%$  lower velocity dispersion. The same halo in an open universe with  $\Omega_0 = 0.3$  would be  $\sim 14\%$  larger than in the EdS case, with 38% lower central density, and 6% lower velocity dispersion.

Our results demonstrate that the presence of a cosmological constant can influence the internal structure of virialized haloes, particularly in their outer regions. This is true even if we use a conservative estimate of the contribution of the cosmological constant to the mean energy density of the universe, for haloes collapsing at the present. In principle, this effect grows in importance for haloes which are destined to form in the future.

The TIS model has many characteristics in common with the haloes with uniform-density

cores which are expected to form from self-interacting dark matter (SIDM) (Burkert 2000, Davé et al. 2000, Firmani et al. 2000). Since our model describes the final equilibrium state of a collapsing halo and is based on a minimum-energy principle, it may transcend the details of the particle interactions which lead to this equilibrium. If so, then it is reasonable to expect that our TIS solution will be a useful approximation for the equilibrium structure of SIDM haloes. A detailed comparison between the TIS model haloes derived here and the predictions of halo formation in the SIDM model would, therefore, be of interest.

The application of the TIS model presented here to the problem of halo formation in the CDM model, including further comparisons with N-body simulation results, will be described elsewhere. In one such application, the TIS model is shown to provide a good theoretical explanation for the observed rotation curves of dark matter – dominated galaxies and the correlation which has been reported between the maximum velocity on a given rotation curve and the galactocentric radius at which it occurs (Iliev & Shapiro 2001).

## ACKNOWLEDGMENTS

This research was supported in part by NSF grant INT-0003682 from the International Research Fellowship Program and the Office of Multidisciplinary Activities of the Directorate for Mathematical and Physical Sciences to ITI and grants NASA ATP NAG5-7363 and NAG5-7821, NSF ASC-9504046, and Texas Advanced Research Program 3658-0624-1999 to PRS.

## REFERENCES

- Bertschinger E., 1985, *ApJS*, 58, 39  
 Binney J., Tremaine S., 1987, *Galactic Dynamics*. Princeton Univ. Press, Princeton, NJ  
 Bryan G.L., Norman M.L., 1998, *ApJ*, 495, 80  
 Burkert A., 2000, *ApJ*, 534, L143  
 Cole S., Lacey C., 1996, *MNRAS*, 281, 716  
 Davé R., Spergel D.N., Steinhardt P.J., Wandelt B.D., 2000, preprint (astro-ph/0006218)  
 Evrard A.E., Metzler C.A., Navarro J.F., 1996, *ApJ*, 469, 494  
 Firmani C., D’Onghia E., Chincarini G., 2000, preprint (astro-ph/0010497)  
 Gunn J.E., Gott J.R., 1972, *ApJ*, 176, 1  
 Iliev I.T., Shapiro P.R., 2001, *ApJ*, 546, L5  
 Iliev I.T. & Shapiro P.R. 2000, in "The Seventh Texas-Mexico Conference on Astrophysics: Flows, Blows, and Glows," eds. W. Lee and S. Torres-Peimbert, *RevMexAA (Serie de Conferencias)*, in press (astro-ph/0006184)



- Kochanek C.S., 1995, ApJ, 445, 559  
 Lahav O., Lilje P.B., Primack J.R., Rees, M.J., 1991, MNRAS, 251, 128  
 Martel H., 1994, ApJ, 421, L67  
 Martel H., Shapiro P.R., 1998, MNRAS, 297, 467  
 Moore B., Quinn T., Governato F., Stadel J., Lake G., 1999, MNRAS, 310, 1147  
 Navarro J., Frenk C.S., White S.D.M., 1997, ApJ, 490, 493  
 Padmanabhan T., 1993, Structure Formation in the Universe. Cambridge University Press, Cambridge  
 Peebles P.J.E., 1980, The Large Scale Structure of the Universe. Princeton University Press, Princeton  
 Press W.H., Schechter P., 1974, ApJ, 187, 425  
 Shapiro P.R., Iliev I.T., 2000, ApJ, 542, L1  
 Shapiro P.R., Iliev I.T., Raga A.C., 1999, MNRAS, 307, 203 (Paper I)  
 Shapiro P.R., Martel H., Iliev I.T., 2001, in preparation  
 Spergel D.N., Steinhardt P.J., 2000, Phys.Rev.Lett., 84, 3760  
 Wang L., Steinhardt P.J., 1998, ApJ, 508, 483

## APPENDIX A: APPLICATION OF THE SELF-SIMILAR, SPHERICAL INFALL SOLUTION AT EARLY TIMES IN A LOW-DENSITY UNIVERSE

The self-similar cosmological infall solution of Bertschinger (1985) can be generalized to the case of a low-density universe at early times by simple scalings of the variables. At early times,  $\Omega(z) \approx 1$ , and both the background universe and density fluctuations evolve approximately as in an EdS universe. Therefore, the self-similar infall solution will be approximately valid. Consider the spherical mass shell which is just turning around at some redshift  $z$ . Let the radius of this shell be  $r_{\text{ta}}$ . According to the top-hat solution applied to this spherical shell, the mass  $m_{\text{ta}}$  enclosed by this shell is just

$$m_{\text{ta}} = \frac{4}{3}\pi r_{\text{ta}}^3 \rho_b(z)(1 + \delta_m), \quad (\text{A1})$$

where  $\rho_b(z)$  is the mean background matter density at redshift  $z$  and  $(1 + \delta_m)$  is the average overdensity inside this sphere at its epoch of maximum expansion. At early times, for which the behaviour approaches that of an EdS universe,  $(1 + \delta_m) = 9\pi^2/16$  and  $\rho_b(z) = \rho_{\text{crit}}(z) = 3H^2(z)/(8\pi G)$ . However, for a low-density universe at high redshift, the Friedmann equation (5) simplifies to

$$H^2(z) = H_0^2 \Omega_0 (1 + z)^3, \quad (\text{A2})$$

so

$$\rho_{\text{crit}}(\Omega_0, z) = \Omega_0 \rho_{\text{crit,EdS}}(z). \quad (\text{A3})$$

Therefore, if we fix the mass inside  $r_{\text{ta}}$  at redshift  $z$ , then we must take a different value for the radius  $r_{\text{ta}}$  for the EdS and low-density universes, according to equations (A1) and (A3), which yields

$$r_{\text{ta}}(z)/r_{\text{ta,EdS}}(z) = [\rho_{\text{crit}}(\Omega_0, z)/\rho_{\text{crit,EdS}}(z)]^{-1/3} = \Omega_0^{-1/3}. \quad (\text{A4})$$

Consider now the mass within a sphere whose radius  $r$  at this redshift  $z$  is a fixed fraction  $\lambda_B$  [in the notation of Bertschinger (1985), where we have added the subscript “B” to this dimensionless radius coordinate to distinguish it here from the unrelated quantities  $\lambda_0$  and  $\lambda(t)$  used elsewhere in this paper to refer to the cosmological constant in units of the critical density, as measured at the present and at time  $t$ , respectively] of the radius  $r_{\text{ta}}$ ,

$$m(\lambda_B, z) = m_{\text{ta}}(z) \frac{M(\lambda_B)}{1 + \delta_m}, \quad (\text{A5})$$

where  $M(\lambda_B)$  is a dimensionless function of  $\lambda_B$  only, for which  $M(1) = 1 + \delta_m$ . According to equation (A5), if we fix the mass  $m_{\text{ta}}$  inside  $r_{\text{ta}}$  at redshift  $z$  when comparing the EdS and low-density universe solutions, we must also have the same mass  $m(\lambda_B, z)$  inside any  $\lambda_B$  in the two solutions. In that case, the radius  $r$  for any  $\lambda_B$  must correspondingly relate to the radius  $r_{\text{EdS}}$  which encloses the same mass at the same redshift, according to

$$r(\lambda_B) = r_{\text{EdS}}(\lambda_B) \Omega_0^{-1/3}. \quad (\text{A6})$$

The age of a low-density universe at a given redshift is related to the age of an EdS universe at the same redshift according to the solutions of the Friedmann equation for these two cases. Equation (A2) is easily integrated analytically to yield the result for high redshift,

$$t(\Omega_0, z) = t_{\text{EdS}}(z) \Omega_0^{-1/2}. \quad (\text{A7})$$

This determines the scaling of velocities in the infall solution, as follows. At any  $\lambda_B$ , the velocity scales as

$$v \propto \frac{r}{t} \quad (\text{A8})$$

Equations (A6) – (A8) yield

$$v(\lambda_B) = v_{\text{EdS}}(\lambda_B) \Omega_0^{1/6}. \quad (\text{A9})$$

## APPENDIX B: ANALYTICAL FITTING FORMULAE FOR THE DEPENDENCE OF THE TIS HALO DIMENSIONLESS PARAMETERS ON $\theta$ AND THE DEPENDENCE OF THE DENSITY PROFILE ON THE DIMENSIONLESS RADIUS $\zeta$

Analytical fitting formulae which closely approximate the numerical results for the dimensionless TIS parameters will make applications of our TIS model much more convenient. We have derived such fitting formulae for two overlapping intervals of  $\theta$ , with different fractional errors in these two intervals, as follows.

In the currently most relevant cosmological range,  $0 \leq \theta \leq 0.123$ , the fits are given by

$$\zeta_t = 29.4003 + 11.4652\theta - 13.8428\theta^2 - 12.8453\theta^3, \quad (\text{B1})$$

$$\alpha = 3.7296 - 0.866069\theta + 1.92742\theta^2 - 1.70326\theta^3, \quad (\text{B2})$$

$$\eta_{\text{TIS}} = 0.554384 - 0.45529\theta + 0.21258\theta^2 + 0.02128\theta^3, \quad (\text{B3})$$

$$\mathcal{R} = 513.842 + 282.031\theta - 193.617\theta^2 - 748.254\theta^3, \quad (\text{B4})$$

$$\tilde{\rho}_\lambda = 0.00123263\theta - 0.00385345\theta^2 + 0.00579887\theta^3, \quad (\text{B5})$$

$$\tilde{M}_t = 61.485 + 23.8887\theta - 32.9854\theta^2 - 14.0272\theta^3. \quad (\text{B6})$$

The relative errors of these fits are  $< 0.01\%$  (except for the fit to  $\tilde{\rho}_\lambda$ , for which the relative error as  $\theta \rightarrow 0$  is higher, since the exact solution has a slightly different slope at  $\theta = 0$  from that of the fitting formula,  $\tilde{\rho}_\lambda \rightarrow a\theta$ , where  $a \approx 0.001217$ . However, for  $\theta < 0.005$  where the above fit for  $\tilde{\rho}_\lambda$  is not perfect, the departure from the result for the EdS case is negligible anyway.)

The fits in the full allowed range  $0 \leq \theta \leq 0.5$  are given by

$$\zeta_t = 29.3893 + 12.0474\theta - 20.752\theta^2 + 11.732\theta^3, \quad (\text{B7})$$

$$\alpha = 3.72913 - 0.843068\theta + 1.71017\theta^2 - 1.20963\theta^3, \quad (\text{B8})$$

$$\eta_{\text{TIS}} = 0.554437 - 0.45804\theta + 0.23999\theta^2 - 0.04279\theta^3, \quad (\text{B9})$$

$$\mathcal{R} = 513.366 + 306.812\theta - 478.871\theta^2 + 222.726\theta^3, \quad (\text{B10})$$

$$\tilde{\rho}_\lambda = 10^{-3}(1.1156\theta - 2.6093\theta^2 + 2.1242\theta^3), \quad (\text{B11})$$

$$\tilde{M}_t = 61.4683 + 24.782\theta - 43.8578\theta^2 + 25.8869\theta^3. \quad (\text{B12})$$

The relative errors of these fits are  $< 0.1\%$  (again with the exception of the fit for  $\tilde{\rho}_\lambda$ ).

In Paper I we obtained a simple analytical fit to the TIS density profile, as follows:

$$\tilde{\rho}(\zeta) = \frac{A}{a^2 + \zeta^2} - \frac{B}{b^2 + \zeta^2}, \quad (\text{B13})$$

for  $\zeta \leq \zeta_t$ , with

$$(A, a^2, B, b^2)_{TIS} = (21.38, 9.08, 19.81, 14.62). \quad (\text{B14})$$

This fit is accurate to within 3% inside the virial radius for  $\lambda_0 = 0$ . In the presence of a cosmological constant, the dimensionless profile varies, as described above. Nevertheless, for  $\lambda_0 < 0.9$  and haloes that collapse by  $z = 0$ , the fit still has accuracy of better than 3%. Overall the fit deteriorates a bit, however, by slightly overestimating  $\tilde{\rho}$  at all radii.

The corresponding fit to the TIS halo circular velocity profile (i.e. the rotation curve), obtained simply by integrating equation (B13), is

$$v_c(r) = \sigma_V \left\{ A - B + \frac{r_0}{r} \left[ bB \arctan\left(\frac{r}{br_0}\right) - aA \arctan\left(\frac{r}{ar_0}\right) \right] \right\}^{1/2} \quad (\text{B15})$$

(Iliev & Shapiro 2001). This fit to  $v_c(r)/\sigma_V$  is good to  $< 1\%$  for  $\lambda_0 = 0$ , and for  $r < 2r_t/3$  if  $\lambda_0 \neq 0$ , while at larger radii, depending on  $\lambda_0$  and  $z_{\text{coll}}$ , the error could be larger but is not greater than 6% at  $r_t$ , even for  $\lambda_0 = 0.9$  and  $z_{\text{coll}} = 0$ . Most of the departure of the exact circular velocity profile from this fit is due to the  $\rho_\lambda$ -dependent correction factor in  $v_c$ , which was omitted here for simplicity. In Iliev & Shapiro (2001), we apply the TIS model to explain the observed rotation curves of dark matter-dominated galaxies and the statistical correlations amongst their rotation curve parameters for different mass haloes collapsing at different epochs in the CDM model for different background cosmologies.